Proceedings of the 53rd Hawaii International Conference on System Sciences | 2020

Analytical Method for Energy Storage Sizing and Reliability Assessment for Power Systems with Variable Generation

Abdullah Alamri
Georgia Institute of Technology
aalamri6@gatech.edu

Maad AlOwaifeer
Georgia Institute of Technology
maad@gatech.edu

A.P Sakis Meliopoulos
Georgia Institute of Technology
sakis.m@gatech.edu

Abstract

This paper presents a mixed integer linear program (MILP) to optimally size power and energy of energy storage systems (ESSs). The sizing model takes into account conventional generation (CG) operation constraints in addition to seasonal and locational wind speed and solar radiation variations, and variable generation (wind turbine systems (WTSs) and solar cell generators (SCGs)) forced outages. Subsequently, the outcomes of the ESS sizing model are inputted to the probabilistic production method (PCC) to assess the reliability of the integrated system. All aforementioned analyses have been applied to a system with different penetration levels. The method is demonstrated with case studies on a system consisting of 10 CG units and VG penetration levels of 20% and 30%. For each penetration level, ESS sizing is computed and then reliability assessment is performed.

Nomenclature

SCG	Solar cell generator
SF	Solar farm
WTS	Wind turbine system
WF	Wind farm
CG	Conventional generation
ESS	Energy storage system
q_{SCGi}	i^{th} SCG forced outage rate
G_h	Historical solar radiation data (W/m^2)
G_{std}	Solar radiation in the standard environment (W/m^2)
R_c	A certain radiation point set usually as 150 W/m^2
$P_{SCG.rated}$	SCG rated power (MW)
$MTTR_{SCG}$	SCG mean time to repair (hrs.)
$MTTF_{SCG}$	SCG mean time to failure (hrs.)
N_{SCG}	Total number of SCGs in a SF
N_{SF}	Total number of SFs
q_{WTSi}	i^{th} WTS forced outage rate
$\rho_{SG}(p_{SCG})$	PDF of SCG power output
ρ_{SFA} (c_{SF})	PDF of SF availability
ρ_{SFG} (p_{SF})	PDF of SF power output
F_{SFG} (p_{SF})	CDF of SF power output
v_{ci} /v_{co} /v_{rated}	Cut-in/ cut-out/ rated speeds (m/s)
$MTTR_{WTS}$	WTS mean time to repair (hrs.)
$MTTF_{WTS}$	WTS mean time to failure (hrs.)
$P_{WTS.rated}$	WTS rated power (MW)
N_{WTS}	Total number of WTSs in a WF
N_{WF}	Total number of WFs
$\rho_{WG}(p_{WTS})$	PDF of WTS power output
ρ_{WFA} (c_{WF})	PDF of WF availability
ρ_{WFG} (p_{WF})	PDF of WF power output
F_{WFG} (p_{WF})	CDF of WF power output
r	Index for the available SCGs/WTSs in a SF/WF
q_q	g^{th} CG forced outage rate
G	Total number of CGs
UT_q/DT_q	Minimum up/down times of a CG (hrs.)
SU_g/SD_g	Startup/shutdown limit of a CG (MWh^{-1})
RU_q/RD_q	Ramp up/down rate of a CG (MW)
CT_g	Cold start time (hrs.)
P_g^{max}/P_g^{max}	Max./min. generation limit of a CG (MW)
T	Time of simulation (hrs.)
H	Historical data size (hrs.)
η_{ch}/ η_{dis}	Charging/Discharging efficiency of ESS
d	ESS energy capacity capital cost ($/MWh)
e	ESS power capacity capital cost ($/MW)
π	Price of wasted VG power ($/MW)
R	The reserve requirement (MW)
D_t	Demand at time t (MW)
Decision variables (all at time t)	
$x_{g,t}$	A binary variable of the g^{th} CG status (1: ON, 0: OFF)
$s_{g,t}$	A binary variable of the g^{th} CG startup status (1: turned on, 0: otherwise)
$z_{g,t}$	A binary variable of the g^{th} CG shutdown status (1: turned off, 0: otherwise)
α_t	A binary variable to prevent ESS simultaneous charging and discharging
$p_{g,t}$	g^{th} CG produced power (MW)
$r_{q,t}$	g^{th} CG reserve provision (MW)
$\overline{P}_{g,t}$	g^{th} CG produced power and reserve upper limit (MW)
$P_{SF,t}$	Solar farm power output (MW)
$P_{WF,t}$	Wind farm power output (MW)
$P_{u,t}$	Unutilized VG power (MW)
$P_{ch,t}$	Power injected into ESS (MW)
$P_{dis,t}$	Power drawn from ESS (MW)
$y_{g,t}$	The g^{th} CG production cost ($)
E_t	ESS level at time t (ESS state of charge)
Decision variables (not function of time)	
E_{ESS}	Energy capacity of ESS (MWh)
P_{ESS}	Maximum discharge/charge rate of ESS (MW)

1. Introduction

The North American Electric Reliability Cooperation (NERC) defines reliability as the ability to serve end-users, or customers, even when unexpected events happen [1]. These unexpected events include forced outages of electric equipment and shortages in generation. This definition divides the reliability into two aspects: adequacy and security. The focus of this work is generation adequacy which is concerned with

URI: https://hdl.handle.net/10125/64106
978-0-9981331-3-3

sufficiency of the electricity resources assessment when adding variable generation (VG) and an energy storage system (ESS).

Renewable energy (RE) sources share has increased globally to meet growing demand [2]. This increment is attributed to their environmental friendliness and the aim to decrease dependence on fossil fuel. However, RE are characterized by intermittency and considered VG. This characteristic affects power systems reliability and operation due to their uncertain power outputs. When referring to VG or RE resources in this work, it strictly means either wind turbine systems (WTSs) or solar cell generators (SCGs). There have been studies on assessing the reliability when adding VG to power systems. These studies are either analytical or Monte Carlo simulation (MCS). MCS is either sequential (SMCS) or non-sequential (NSMCS). For instance, references [3] and [4] developed methods to find the probability density function (PDF) of a number of SCGs/WTSs respectively using both analytical method and MCS. Then, the reliability of a system with VGs was assessed by sampling techniques from the computed PDFs. These models took into account weather predictions and forced outage rates (FORs) of VG units. Reference [5] used hourly mean solar radiation method to predict solar radiation. Then, it assessed reliability using MCS and three-state models (Up-Derated-Down) for both conventional generation (CG) and VG. These are examples of previous works that have been done on modeling VG effect without considering ESSs. Moreover, all these studies were on small-scale systems, hence, it did not include commitment scheduling for CG units. For larger scale systems and in presence of high penetration of VG, the problem of CG unit commitment economic dispatch (UCED) also arises as an important factor. The UCED is an optimization problem that determines the ON/OFF scheduling decisions of CG units satisfying the loading and operational constraints. There have been numerous studies on solving UCED, without considering ESSs. These studies have used different optimization techniques such as dynamic programing, Lagrangian relaxation and mixed integer programming (MIP) [6]-[8]. The focus of this work is mixed integer linear programming (MILP). The optimal ESSs sizing (power and energy capacities) is challenging due to high cost of ESSs, the uncertainty associated with the VG and the dimensionality of the problem.

Different technologies have been used to store energy. These include electrical, thermal, mechanical, and electrochemical [9]. Depending on the technology used, ESSs come in various forms, scales and specifications. There have been studies of ESSs in power systems. In studies with emphasis on reliability, some studies have developed models to assess the impact on reliability given the ESS size (power and energy), while other studies have developed models to determine the optimal ESS sizing and then assess reliability. For instance, reference [10] modeled wind speeds as Weibull distribution and used MCS to assess reliability contribution from ESSs in presence of high penetration of wind generation. However, it considered neither WTS FOR nor optimal ESS sizing. On the other hand, the study in [11] assessed the reliability of hybrid SCG-ESS system using discrete time Markov chain to capture uncertainty in SCG and ESS output. However, it did not consider FOR of SCG. In reference [12], pattern search-based optimization and SMCS were used to optimally size a hybrid VG/ESS power system while meeting certain reliability requirements. Nevertheless, there is a need for a comprehensive model that determines the ESS optimal sizing while accounts for uncertainty in weather prediction, FORs of all VG and CG units, CG operation constraints, and demand and reserve requirements.

This paper formulates the ESS sizing in presence of VG at different penetration levels. The problem is formulated as MILP and considers the following: (1) VG units forced outages, (2) solar radiation and wind speed uncertainty, (3) CGs ramping constraints, maximum/minimum production limits and startup/shutdown period limits, and (4) load and reserve requirements. Firstly, for specific locations, historical seasonal wind speeds and solar radiation data along with WTSs/SCGs FORs and their generation models are used to find power output PDFs of WTSs/SCGs. The PDFs are computed analytically and integrated into the MILP for finding ESS sizing. The objective of the optimization problem is to minimize CGs production, startup and shutdown costs in addition to ESS investment costs (ESS energy and power capacity capital cost, respectively). Once the ESS optimal sizing is computed, a reliability assessment is performed to quantify reliability improvements from the addition of ESS. The reliability assessment is based on a probabilistic method called the probabilistic production costing (PPC) method. The PPC method is a probabilistic simulation method based on the Baleriaux, *et al* method [14], [15]. Formal applications are presented in [16]. The PPC method computes expected operational cost and specific reliability indices: (1) loss of load probability (LOLP), (2) loss of load expectation (LOLE) and (3) expected unserved energy (EUE).

The paper is organized as follows: section 2 provides the problem statement, section 3 describes the VG power output PDFs computational procedures, section 4 provides the formulation of the ESS optimal sizing, section 5 describes the PPC method, section 6 presents a case study and section 7 provides conclusions.

2. Problem Statement

The ESS sizing optimization problem requires the following data:

2.1. Variable Generation Data

The VG is represented by solar farms (SFs) and wind farms (WFs). A SF consists of N_{SCG} number of SCGs. The number of SCGs in the SF defines the solar generation penetration level. For SCG i, where i= 1,…, N_{SCG}, the FOR of SCG$_i$ is denoted by q_{SCGi} and the rated power by $p_{SCG.ratedi}$. The historical data of the solar radiation (G_h) is given, where h=1,2,…,H. The solar radiation data is partitioned into four different groups depending on the season: winter, spring, summer and fall. Also, the SCG power (p_{SCG}) versus solar radiation curve is known. While not necessary, for simplicity in this paper all SCGs are assumed to be exposed to the same solar radiation. Also, we assume that the type of SCGs, and N_{SCG} are identical in each SF.

Similarly, a WF consists of N_{WTS} WTSs. The number of WTSs in the WF defines the wind generation penetration level. For WTSs i, where i= 1,…, N_{WTS}, the FOR is denoted by q_{WTSi} and the rated power by $p_{WTS.ratedi}$. The historical data of the wind speed (V_h) is given, where h=1,2,…,H. The wind speed data is partitioned into four different seasonal groups as in the solar radiation case. Also, the WTS power as a function of the wind speed is also given. Similar to SCGs, in this paper all WTSs in the WF are assumed to be exposed to the same wind speed. Also, we assume that the type of WTSs and N_{WTS} are identical in each WF.

2.2. Conventional Generation Data

The number of CG units is G. The data given for each CG unit includes maximum and minimum power limits, production cost coefficients, minimum up and minimum down times, hot and cold startup costs, cold startup time, mean time to repair and mean time to failure.

2.3. Energy Storage System Sizing Data

The energy and power costs of ESS are given as well as the ESS charging/discharging efficiency.

Given the four partitioned data sets of solar radiation/wind speed of a specific location, it is desired to find the PDF and cumulative distribution function (CDF) of solar radiation/wind speed for each season. Then, using these PDFs and CDFs conditioned on the availability of SCGs/WTSs, the SFs/WFs power output PDFs and CDFs are computed for each season. Once the PDFs and CDFs of SFs/WFs power output of all four seasons are computed, SFs/WFs power samples can be integrated into the ESS sizing optimization problem to represent SFs/WFs forecasted outputs. Then, solving for the ESS sizing gives ESS charging/discharging profile and utilized WFs/SFs power to be inputted to the PPC method in addition to the forecasted load to compute the net equivalent load, as explained in detail later.

3. Computation of SF/WF Generated Power Probability Distribution Function

3.1. SF Probability Distribution Function

This section presents the analysis for a single SF, which is repeated for every SF in the study. For simplicity, the subscript s (s=1,…, N_{SF}) in p_{SFs}, N_{SCGs}, …, etc. is omitted.

For each season's solar radiation historical data set, the first step is to find the PDF of the solar radiation ($\rho_G(g)$). To find $\rho_G(g)$, a histogram is to constructed with appropriate number of bins and subsequently converted the histogram to a PDF using the fact that $\int_{-\infty}^{\infty}\rho_G(g)dg=1$ [3]. Once $\rho_G(g)$ is known, the solar power versus solar radiation curve, conditional upon the availability of the SCG, can be utilized to find the SCG power PDF ($\rho_{SG}(p_{SCG})$). This can be mathematically expressed as in (3.1) [17]:

$$p_{SCG}=\begin{cases} p_{SCG.rated}\left(\dfrac{G_h^2}{G_{std}R_C}\right) & \forall G_h\in[0,R_C) \\ p_{SCG.rated}\left(\dfrac{G_h}{G_{std}}\right) & \forall G_h\in[R_C,G_{std}] \\ p_{SCG.rated} & \forall G_h\in(G_{std},\infty) \end{cases} \quad (3.1)$$

As explained in detail in our previous work [3], the SCG is modeled as a 2-state model: either the unit is available with probability equal to 1−q_{SCGi} and capacity of $p_{SCG.ratedi}$, or unavailable with capacity equal to zero and probability equal to q_{SCGi}. The probability that the SCG is unavailable is computed as follows [18]:

$$q_{SCGi}=\frac{MTTR_{SCGi}}{MTTF_{SCGi}+MTTR_{SCGi}} \quad (3.2)$$

For simplicity in this paper, $p_{SCG.ratedi}$ and q_{SCGi} is assumed identical for all SCGs, hence, the index i is omitted. To find the probability of all possible power output of a SCG, the law of total probability is used as in (3.3):

$$\rho_{SG}(p_{SCG})=\rho_{SG}(p_{SCG}\mid SCG\ is\ UP)(1-q_{SCG}) + \rho_{SG}(p_{SCG}\mid SCG\ is\ DOWN)(q_{SCG}) \quad (3.3)$$

In the case of a SF, there are N_{SCG} SCGs. The probability mass function (PMF) of SF availability ($\rho_{SFA}(c_{SF})$) can be expressed using the binomial distribution as follows:

$$\rho_{SFA}(c_{SF}) = \sum_{r=0}^{N_{SCG}} \binom{N_{SCG}}{r} (1-q_{SCG})^{r} (q_{SCG})^{N_{SCG}-r} \delta(c_{SF} - r\, p_{SCG.rated})$$

The $\rho_{SFG}(p_{SF})$ can be generalized for a SF, i.e., N_{SCG} SCGs. There are three cases for a SF output as follows:

I. For $p_{SF} = 0$, either all SCGs are unavailable or $G_t = 0$, as expressed in (3.4):

$$\rho_{SFG}(0) = \left({q_{SCG}}^{N_{SCG}} + \left(\sum_{r=1}^{N_{SCG}} \binom{N_{SCG}}{r} (1-q_{SCG})^{r} (q_{SCG})^{N_{SCG}-r} \right) F_G(G_t = 0) \right) \delta(p_{SF}) \quad (3.4)$$

II. For $0 < p_{SF} < rp_{SCG.rated}$, the SF generates a percentage of its rated power depending on the number of available SCGs as in (3.5):

$$\rho_{SFG}(rp_{SCG}) = \binom{N_{SCG}}{r} (1-q_{SCG})^{r} (q_{SCG})^{N_{SCG}-r} \rho_{G}(G_t) \quad (3.5)$$

$$\forall G_t \in [0, G_{std}], r = 1, 2, ..., N_{SCG}$$

where p_{SCG} as in equation (3.1)

In case II, $\rho_{SFG}(rp_{SCG})$ is calculated for all possible values of $rp_{SCG} \in (0, rp_{SCG.rated})$ for all r, and eventually summing up all probabilities resulting from equal rp_{SCG} values because of the overlap as r increases.

III. For $0 < p_{SF} < rp_{SCG.rated}$, the probabilities are as in equation (3.6):

$$\rho_{SFG}(r\, p_{SCG.rated}) = \binom{N_{SCG}}{r} (1-q_{SCG})^{r} (q_{SCG})^{N_{SCG}-r} (1-F_G(G_{std})) \delta(p_{SF} - r\, p_{SCG.rated}) \quad (3.6)$$

$$r = 1, 2, ..., N_{SCG}$$

3.2. WF Probability Distribution Function

This section presents the analysis for a single WF, which is repeated for every WF in the study. For simplicity, the subscript w (w=1,…, N_{WF}) in p_{WFw} , N_{WTSw} ,…etc. is omitted.

The method for computing the PDF of each season wind speed ($\rho_V(v)$) is similar to the method used for computing $\rho_G(g)$ [4]. Once $\rho_V(v)$ is known, the WTS curve, conditional upon the availability of the WTS, can be utilized to compute the PDF of the WTS power ($\rho_{WG}(p_{WTS})$). This can be mathematically expressed as follows [19]:

$$p_{WTS} = \begin{cases} p_{WTS.rated} \left(\dfrac{V_t^s - v_{ci}^s}{v_{rated}^s - v_{ci}^s} \right) & \forall V_t \in (v_{ci}, v_{rated}) \\ p_{WTS.rated} & \forall V_t \in [v_{rated}, v_{co}) \\ 0 & \text{otherwise} \end{cases} \quad (3.7)$$

where s equals 1 in this study. Notably, it is assumed in this paper that the WTSs in the WF are arranged in such a way that makes the wake effect negligible.

As explained in detail in our previous work [4], the WTS is modeled as a 2-state model: either the unit is available with probability equal to $1-q_{WTSi}$ and capacity of $p_{WTS.rated}$, or unavailable with capacity equal to zero and probability equal to q_{WTSi}. The probability that the WTS is unavailable is computed as follows [18]:

$$q_{WTSi} = \frac{MTTR_{WTSi}}{MTTF_{WTSi} + MTTR_{WTSi}} \quad (3.8)$$

For simplicity in this paper, q_{WTSi} is assumed identical for all WTSs, hence, the index i is omitted.

To find the probability of all possible WTS power outputs, the law of total probability is used as in (3.9):

$$\rho_{TG}(p_{WTS}) = \rho_{TG}(p_{WTS} \mid WTS\ is\ UP)(1-q_{WTS}) + \rho_{TG}(p_{WTS} \mid WTS\ is\ DOWN)(q_{WTS}) \quad (3.9)$$

In the case of a WF, there are N_{WTS} WTSs. The PMF of WF availability ($\rho_{WFA}(c_{WF})$) can be expressed using the binomial distribution as follows:

$$\rho_{WFA}(c_{WF}) = \sum_{r=0}^{N_{WTS}} \binom{N_{WTS}}{r} (1-q_{WTS})^{r} (q_{WTS})^{N_{WTS}-r} \delta(c_{WF} - p_{WTS.rated})$$

The $\rho_{WFG}(p_{WF})$ can be generalized for a WF, i.e., N_{WTS} WTSs. There are three cases for a WF output:

For $p_{WF} = 0$, either all WTSs are unavailable or V_h falls out the generation zone of a WTS ($V_h \le v_{ci}$, or $V_h \ge v_{co}$), as expressed in equation (3.10):

$$\rho_{WFG}(0) = \left({q_{WTS}}^{N_{WTS}} + \left(\sum_{r=1}^{N_{WTS}} \binom{N_{WTS}}{r} (1-q_{WTS})^{r} (q_{WTS})^{N_{WTS}-r} \right) A \right) \delta(p_{WF}) \quad (3.10)$$

$$\text{where } A = \int_{-\infty}^{v_{ci}} \rho_V(v)\, dv + \int_{v_{co}}^{\infty} \rho_V(v)\, dv$$

I. For $0 < p_{WF} < rp_{WTS.rated}$, the WF generates a percentage of its rated power depending on the number of available WTSs as expressed in (3.11):

$$\rho_{WFG}(rp_{WTS}) = \binom{N_{WTS}}{r} (1-q_{WTS})^{r} (q_{WTS})^{N_{WTS}-r} \rho_{v}(V_h) \quad (3.11)$$

$$\forall V_h \in (v_{ci}, v_{rated})$$

where p_{WTS} is as in equation (3.7)

For case II, $\rho_{WFG}(rp_{WTS})$ is calculated for all possible values of $rp_{WTS} \in (0, rp_{WTS.rated})$ for all r, and eventually summing up all probabilities resulting from equal rp_{WTS} values because of the overlap as r increases.

II. For $0 < p_{WF} < rp_{WTS.rated}$, the probabilities are expressed as in equation (3.12):

$$\rho_{WFG}(r\,p_{WTS.rated}) = \binom{N_{WTS}}{r}(1-q_{WTS})^{r}(q_{WTS})^{N_{WTS}-r}(B)\,\delta(p_{WF}-r\,p_{WTS.rated}) \quad r=1,2,...,N_{WTS} \tag{3.12}$$

where $B = \int_{v_{rated}}^{v_{co}} \rho_V(v)dv = F_V(v_{co}) - F_V(v_{rated})$

An important step when applying the ESS sizing, is to represent the uncertainty in the SFs and WFs power. The uncertainty is represented in the aforementioned CDFs of the SF and WF of each season.

4. Energy Storage System Sizing Optimization Formulation

The ESS sizing optimization problem is formulated as a modified UCED problem. The UCED optimization problem objective is to minimize the production costs in addition to the startup and shutdown costs. The UCED optimization problem should meet certain constraints. These constraints include load and reserve requirements, maximum and minimum production limits, minimum up and down time limits and ramp up and ramp down limits. The ESS investment and operational costs (power and energy) are added to the aforementioned costs while meeting all previously mentioned constraints, in addition to the ESS dynamics constraints, as discussed in detail next. The UCED in this work has been proposed in [7] and explained in [8]. The ESS sizing is explained in [20].

The objective function is linear and is in the form of:

$$min \sum_{t\in T}\sum_{g\in G}(y_{g,t} + SUcost_{g,t} + z_{g,t}SDcost_g) + \pi\sum_{t\in T}(P_{u,t} - P_{ch,t}) + dE_{ESS} + eP_{ESS}$$

The objective function is to minimize CG production cost, startup and shutdown costs, and the ESS energy capacity and power rating capital costs. Here, we add a penalty for not utilizing VG (SFs and WFs) power. The penalty is on the VG that neither serves the load directly nor charges the ESS. All the terms in the objective function are linear. The production and the startup costs are originally non-linear but are linearized in our formulation. The production cost of CG is quadratic and is in the form of:

$$a_g p_{g,t}^2 + b_g p_{g,t} + c_g$$

Where a_g, b_g and c_g are the cost coefficients of the g^{th} CG. We use piecewise segments to linearize the quadratic cost function as shown in [21]. Each segment j is characterized by a starting point (x_j,c_j) and a slop m_j. Once these values are set, the quadratic cost function for a CG is replaced by the following set of constraints:

$$y_{g,t} \ge m_j(p_{g,t} - x_j) + c_j \qquad j=1,2,...,J \tag{4.1}$$

In regards to the startup cost, it is approximated as a staircase function as explained in [22] and formulated as in (4.2) for each CG g at time t. Assuming for a CG g, there are *s-value* staircase, each value represents the cost k_τ (τ=1,2,…,S), where $k_{\tau+1} > k_\tau$. Then, if the CG g has been off for τ hours before time t, the incurred startup cost $SUcost_{g,t}$ will be k_τ.

$$SUcost_{g,t} \ge k_\tau\left(x_{g,t} - \sum_{i=1}^{t_g^\tau} x_{g,t-i}\right) \qquad \tau=1,2,...,S \tag{4.2}$$

The other set of constraints of the ESS sizing problem starts with the CG constraints:

$$x_{g,t} - x_{g,t-1} = s_{g,t} - z_{g,t} \qquad \forall g\in G, \forall t\in T \mid t=1 \tag{4.3}$$

Constraint (4.3) captures changes in CG status (ON→OFF or OFF→ON) between time step t and t−1. Variables $s_{g,t}$ and $z_{g,t}$ capture CG transitions OFF→ ON and ON→OFF, respectively. Both $s_{g,t}$ and $z_{g,t}$ are determined by knowing $x_{g,t}$ and $x_{g,t-1}$. $s_{g,t}$ and $z_{g,t}$ cannot be both 1 at the same time: either there is no transition where both variables equal 0, or there is a transition where one of them is 1.

Constraint (4.4) insures that a CG generates at minimum P_g^{min} when ON and 0 when OFF.

$$p_{g,t} \ge P_g^{min}\, x_{g,t} \qquad \forall g\in G, \forall t\in T \tag{4.4}$$

Constraint (4.5) insures that a CG generates maximum P_g^{max} when it is ON and does not exceed the shutdown rate when it is off at t+1.

$$p_{g,t} \le \bar{p}_{g,t} \le P_g^{max} x_{g,t} + (SD_g - P_g^{max})\, z_{g,t+1} \qquad \forall g\in G, \forall t\in T \tag{4.5}$$

Note that $\bar{p}_{g,t} = p_{g,t} + r_{g,t}$.

At any instant t, the CG units should provide reserve (R) and serve the demand. R is calculated as a percentage of the peak load plus the largest CG unit capacity, constraint (4.6) insures that the demand and reserve requirements are met:

$$\sum_{g\in G}\bar{p}_{g,t} \ge D_t + R \qquad \forall t\in T \tag{4.6}$$

Next, demand and energy charging into the ESS at time t must be met by CGs, SFs, WFs, and ESS:

$$\sum_{g\in G} p_{g,t} + \sum_{s=1}^{N_{SF}} p_{SFs,t} + \sum_{w=1}^{N_{WF}} p_{WFw,t} + p_{dis,t} = D_t + p_{ch,t} \quad \forall t \in T \quad (4.7)$$

Once a CG unit is turned ON/OFF, it has to be ON/OFF for at least a period of time. These are referred to as the minimum up time (UT_g) and minimum down time (DT_g) constraints. Constraint (4.8) and (4.9) insure that the transition from ON→OFF/OFF→ON has occurred at most once during the UT_g /DT_g period, respectively.

$$\sum_{i=t-UT_g+1}^{t} s_{g,i} \le x_{g,t} \qquad \forall t \in T, \forall g \in G \quad (4.8)$$

$$\sum_{i=t-DT_g+1}^{t} s_{g,i} \le 1 - x_{g,t-DT_g} \quad \forall t \in T, \forall g \in G \quad (4.9)$$

When a CG is ON, the ramp up/down limits are up to RU_g/RD_g. However, a transition from ON→OFF or OFF→ON at t and t+1, force these limits to be SD_g/SU_g.

$$\bar{p}_{g,t} - p_{g,t-1} \le SU_g \; s_{g,t} + RU_g \; x_{g,t-1} \quad (4.10)$$

$$p_{g,t-1} - p_{g,t} \le SD_g \; z_{g,t} + RD_g \; x_{g,t} \quad (4.11)$$

The VG (SFs and WFs) set of constraints determine the expected output of SCGs and WTSs taking into consideration the uncertainty associated with this type of generation. Earlier in section 2, G_h and V_h, were partitioned to four groups depending on the season. Subsequently, we introduced how to analytically compute $\rho_{SFGs}(p_{SFs})/F_{SFGs}(p_{SFs})$ and $\rho_{WFGw}(p_{WFw})/F_{WFGw}(p_{WFw})$. Starting with SCGs in a SF, once the $F_{SFGs}(p_{SFs})$ of each season is computed, uniform random numbers are generated, U_t ~unif$(0,1)$. The number of the generated random numbers equals T, the simulation period. T is chosen to represent the four seasons with each season representing T/4 hrs. In our study, T equals to four weeks (672 hrs.) and each season is represented by a week (168 hrs.). Then, these random numbers are used to compute the power using the inverse transform method. The power computed here is the maximum output of every SF at instant t as follows:

$$p_{SFs\max,t} = F^{-1}_{SFGs}(U_t) \qquad s = 1,...,N_{SF} \quad (4.12)$$

Constraint (4.13) represents the SF production limits:

$$0 \le p_{SFs,t} \le p_{SFs\max,t} \qquad s = 1,...,N_{SF} \quad (4.13)$$

Similarly, once $F_{WFGw}(p_{WFw})$ of each season is computed, uniform random numbers are generated, U_t ~unif$(0,1)$. Then, they are used to compute the power using the inverse transform method. The power computed is the maximum output of the WF at instant t as follows:

$$p_{WFw\max,t} = F^{-1}_{WFGw}(U_t) \quad w = 1,...,N_{WF} \quad (4.14)$$

Constraint (4.15) represents the WF production limits:

$$0 \le p_{WFw,t} \le p_{WFw\max,t} \qquad w = 1,...,N_{WF} \quad (4.15)$$

It is desirable to utilize all the VG either to serve the load directly or to charge the ESS. However, this may not be always possible. Hence, we introduce a variable that represents the unutilized VG generation for it to be penalized in the objective function:

$$p_{u,t} = \sum_{s=1}^{N_{SF}} p_{SFs\max,t} - \sum_{s=1}^{N_{SF}} p_{SFs,t} + \sum_{w=1}^{N_{WF}} p_{WFw\max,t} - \sum_{w=1}^{N_{WF}} p_{WFw,t} \quad (4.16)$$

Constraints (4.17) to (4.23) dictate the operation of ESS; i.e., how ESS charges/discharges and limits of both ESS energy and power. These constraints are key factors in determining the optimal ESS sizing. Constraint (4.17) determines the state of charge (SOC) of the ESS between two consecutive time intervals. Constraints (4.18), (4.19) and (4.20) are the ESS energy, charging and discharging power limits, respectively. Notably, E_{ESS} and P_{ESS} are decision variables. Constraints (4.21) and (4.22) are to avoid simultaneously charging and discharging the ESS. M here is a large number, e.g., 1000 MW. In this work, while not necessary, P_{ESS} is restricted to be less than or equal to one third of E_{ESS}, as in constraint (4.23).

$$E_{t+1} = E_t + \eta_{ch} p_{ch,t} - \frac{p_{dis,t}}{\eta_{dis}} \quad \forall t \in T \quad (4.17)$$

$$0 \le E_t \le E_{ESS} \quad \forall t \in T \quad (4.18)$$

$$0 \le P_{ch,t} \le P_{ESS} \quad \forall t \in T \quad (4.19)$$

$$0 \le P_{dis,t} \le P_{ESS} \quad \forall t \in T \quad (4.20)$$

$$0 \le P_{ch,t} \le \alpha_t M \quad \forall t \in T \quad (4.21)$$

$$0 \le P_{dis,t} \le (1-\alpha_t) M \quad \forall t \in T \quad (4.22)$$

$$p_{ESS} \le \frac{E_{ESS}}{3} \quad (4.23)$$

The last ESS constraint is to restrict the ESS charging power to be less than or equal to p_u.

$$p_{ch,t} \le p_{u,t} \quad \forall t \in T \quad (4.24)$$

5. Reliability Assessment Using the Probabilistic Production Costing

The PPC method uses a series of convolutions to project CG system production costs, and to assess reliability [14]-[16]. The CG units serve a given load represented with a load duration curve (probabilistic model of the load). The loading of CGs follows economic dispatch, i.e., the lowest CG cost is loaded

Table I. Conventional Generation data

g	P^{max} (MW)	P^{min} (MW)	*a* ($/MW^2)	*b* ($/MW)	*c* ($)	DT (hrs.)	UT (hrs.)	Hot Start cost ($)	Cold Start cost ($)	CT (hrs.)	MTTF (hrs.)	MTTR (hrs.)
1	455	150	4.80E-04	16.19	1,000	8	8	4,500	9,000	5	967	33
2	455	150	3.10E-04	17.26	970	8	8	5,000	10,000	5	967	33
3	130	20	0.00200	16.60	700	5	5	550	1,100	4	960	40
4	130	20	0.00211	16.50	680	5	5	560	1,120	4	960	40
5	162	25	0.00398	19.70	450	6	6	900	1,800	4	960	40
6	80	20	0.00712	22.26	370	3	3	170	340	2	1,960	40
7	85	25	7.90E-04	27.74	480	3	3	260	520	2	1,960	40
8	55	10	0.00413	25.92	660	1	1	30	60	0	969	31
9	55	10	0.00222	27.27	665	1	1	30	60	0	969	31
10	55	10	0.00173	27.79	670	1	1	30	60	0	969	31

first. The original PPC method is modified in presence of VG (SFs and WFs) and ESS. In this case, the CGs serve the composite load or the effective load, i.e. load minus VG and ESSs outputs. The composite load duration is the load minus the summation of VG output and the ESS discharge/charge power, referred to it as the equivalent load duration curve (ELDC). A description of the PPC is included in the following subsections.

5.1. Conventional Generation Units

A CG unit is modeled as a 2-state model, either available with probability 1-q_g and capacity equals to P_g^{max} or unavailable with probability q_g.

5.2. Equivalent Load Representation

The ELDC is computed using the forecasted load, the SFs and WFs power output consumed directly by the demand, and ESS discharge/charge power. The ELDC is computed as follows:

$$\text{ELDC} = \text{Load} - \text{Expected VG Power} - \text{ESS power} \quad (5.1)$$

Subsequently, the resultant curve is converted to an inverted probability distribution function (IPDF) as explained in [16]. The IPDF is a LDC with inverted axes, i.e., the horizontal axis is the load in MW and the vertical axis is probability.

5.3. Reliability Assessment

As mentioned before, the PPC method uses series of convolutions. The resultant curves from these series of convolutions are used to calculate reliability indices: LOLP, LOLE and EUE. Once the IPDF curve is constructed, the PPC method uses convolution between the equivalent loads and CGs output the PDF for the load to be served by the next CG unit. This convolution operation is expressed in (5.2):

$$L_g(l) = (1-q_g)\,L_{g-1}(l + p_g^{max}) + q_g\,L_{g-1}(l) \quad (5.2)$$

where $g = 1, 2, \ldots G$, and L_g is the curve after CG g is loaded (L_0 = IPDF). The CGs units are loaded sequentially to simulate economic dispatch, i.e., lowest cost first. Once all CGs are loaded, the LOLP is the value of last curve (L_G) at zero, as in (5.3):

$$LOLP = L_G(0) \quad (5.3)$$

Once LOLP is computed, LOLE is computed as LOLE = LOLPx8760 (hrs./year). Finally, EUE is the area under the L_G curve expressed as in (5.4):

$$EUE = T \int_0^{Peak\ Load} L_G(l)\,dl \quad (5.4)$$

6. Case Study

Hourly solar radiation and wind speed data for 6 years of Texas is collected [23],[24]. The SCGs/WTSs in the SFs/WFs have the same specifications. The VG penetration levels are 20% and 30% of the total CG installed capacity. There are 2 WFs and 2 SFs in the study. The WFs and SFs contribute equally to each penetration level. For instance, if the VG penetration level is 20%, 5% is the contribution of each WF/SF. N_{SCG} and N_{WTS} are dependent on the considered VG penetration level. Starting with the SFs, there are N_{SCG} SCGs in each SF and each SCG has $p_{SCG.rated}$ = 5 MW, G_{std} = 1 kW/m^2, and R_C = 150 W/m^2. q_{SCG} = 0.15, $MTTF_{SCG}$ = 950 hrs., and $MTTR_{SCG}$ = 167.7 hrs. On other hand, the Areva Multibird M5000 WT specifications are utilized to perform the analysis of the case study [23]. These specifications are: $p_{WTS.rated}$ = 5 MW, v_{ci} = 4 m/s, v_{rated} = 12.5 m/s, *and* v_{co} = 25 m/s. q_{WTS} is assumed to be 0.15, $MTTF_{WTS}$ = 950 hrs. and $MTTR_{WTS}$ = 167.7 hrs. The ESS technology chosen for the ESS sizing is lead-acid with the following specifications: $\eta_{ch} = \eta_{dis}$ = 80%, and energy and power capital cost of 330 k$/MWh and 400 k$/MW, respectively [25]. The time of simulation, T, is 672 hrs. and e and d are computed to reflect the cost of the ESS T. The assumptions made to reflect it over T are expected life time of 20 years and discount rate of 5%.

Using these assumptions, these costs are e=2,037 \$/MWh and d = 2,469 \$/MW. The price penalty on unutilized VG, π, equals 80 \$/MWh. Finally, the test system consists of: (1) 10 CGs with specifications shown in Table I [26], (2) 2 SFs, (3) 2 WFs, and (4) load with the p.u. data taken from the IEEE-RTS with a base of 1,150 MW [27].

6.1. SFs/WFs Power PDF/CDF Results

SFs and WFs power output PDFs and CDFs were computed for all seasons and for the two penetration levels. Taking 30% penetration level as an example, Figure 1 and Figure 2 show comparison between the two SFs output. These figures show that SF1 has lower zero output probabilities in both seasons than SF2, and the similar results were observed for the fall and spring seasons. On the other hand, Figure 3 and Figure 4 compare the output of WF1 and WF2 in winter and summer. WF2 has lower probabilities of having zero output in these seasons and similar results were observed the remaining seasons.

6.2. ESS Sizing Results

Table II shows the optimal P_{ESS}, and E_{ESS} as well as the resultant ESS cost for the two penetration levels over the simulation period. Comparing the ESS sizing at 30% and 20%, P_{ESS} and E_{ESS} at 30% were significantly larger than P_{ESS} and E_{ESS} at 20%. This might be attributed to the significant increase in penetration (10% more) that resulted in more VG utilized and a change in CGs operation to reduce the overall cost while maintaining the operational constraints.

To compute reliability the same analysis was applied first without ESS and VG (base case with just CG) and then with only VG (no ESS). Taking the 30% penetration level as an example, Figure 5 shows the charging/discharging and SOC profiles of the ESS. Figure 6 shows the unutilized VG power with and without ESS. The ESS clearly decreased the unutilized energy significantly and resulted in reducing the total cost of the system from \$ 7,946,000 to \$7,341,000 and improved the system reliability as well.

Table II. ESS Sizing Results

VG %	P_{ESS} (MW)	E_{ESS} (MWh)	ESS Cost (\$)
30%	52.60	157.79	451,287.60
20%	9.81	29.46	84,230.91

6.3. Reliability Assessment Results

Table III shows the reliability assessment and cost projection of the two penetration levels with/without ESS. Compared to the base case, the improvement ranged from 35 % to 63% in LOLP and LOLE in the presence of VG and ESS while ranged from 22% to 43% in presence of only VG. similarly, the EUE improvement ranged from 36% to 54% in presence of only VG while the improvement ranged from 54% to 74% in the case of VG and ESS. The total cost followed the same pattern as the EUE and LOLP.

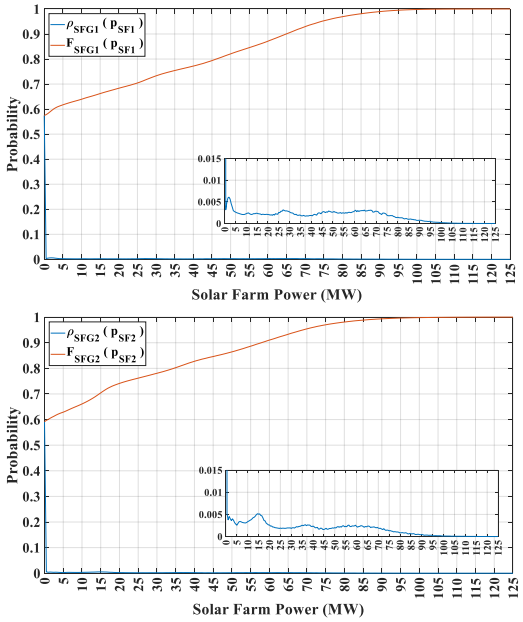

Figure 1. Winter season PDFs and CDFs of SF1 (above) and SF2 (below) at 30% penetration level

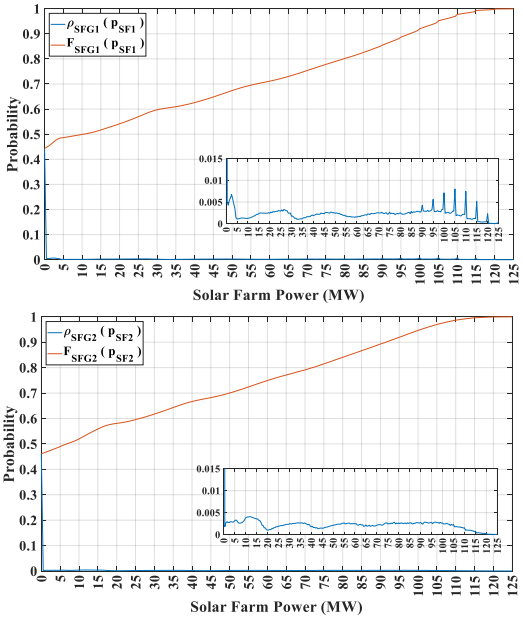

Figure 2. Summer season PDFs and CDFs of SF1 (above) and SF2 (below) at 30% penetration level

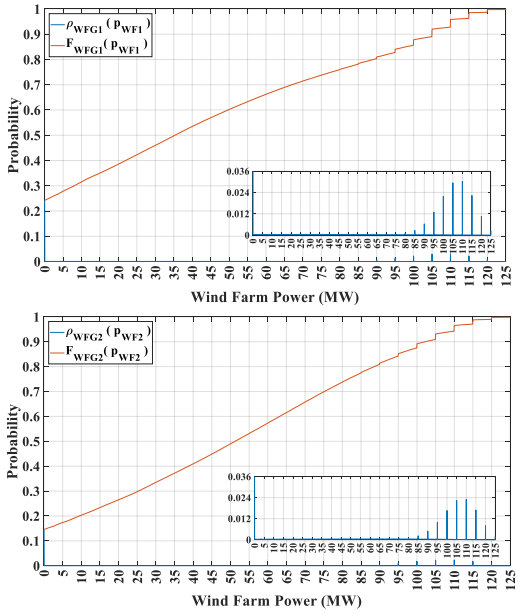

Figure 3. Winter season PDFs and CDFs of WF1 (above) and WF2 (below) at 30% penetration level

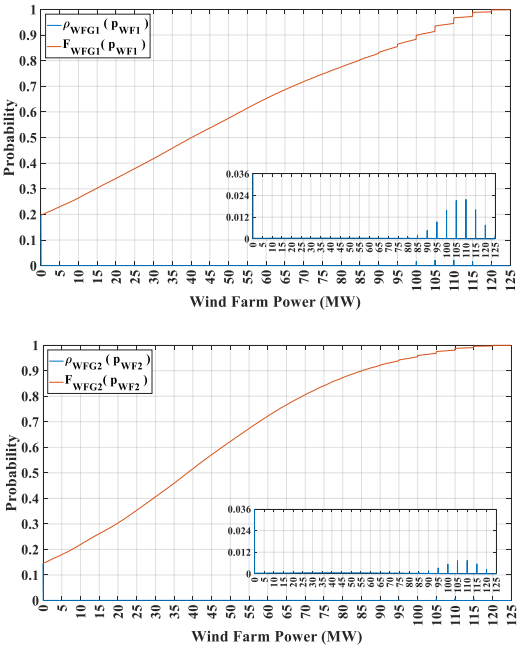

Figure 4. Summer PDFs and CDFs of WF1 (above) and WF2 (below) at 30% penetration level

7. Conclusions

This paper presented a MILP model for optimal ESS sizing that considers VG units forced outages, seasonal and locational variation of wind speed and solar radiation and different penetration levels. Subsequently, the PPC method was used to assess the ESS impact on reliability. The results indicate that for the specific system considered, ESS improved both LOLP index and the EUE index, and reduced the total expected cost.

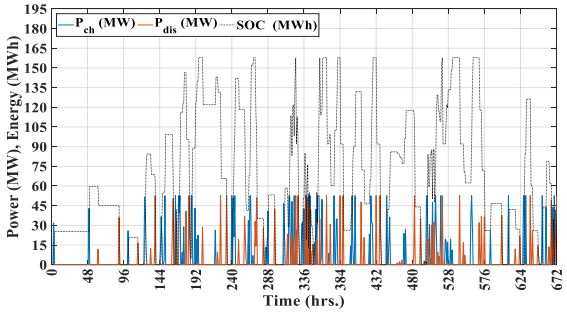

Figure 5. ESS power and energy profiles at 30% penetration

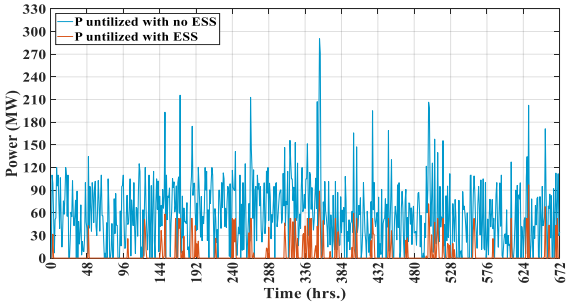

Figure 6. Unutilized VG at 30% penetration (with/without ESS)

Table III. Reliability Assessment Results

Case	VG %	LOLP	LOLE (hrs./y)	EUE (MWh)	Total Cost (k$)
Base	0%	0.00054	4.73	43.11	9,184
VG only	20%	0.00042	3.68	27.46	8,470
	30%	0.00031	2.72	19.92	7,946
VG+ESS	20%	0.00035	3.07	19.71	8,045
	30%	0.00020	1.75	11.05	7,341

8. References

[1] North American Electric Reliability Cooperation (NERC), 2019. [Online]. Available: https://www.nerc.com/AboutNERC/exec/Pages/FAQ.aspx.

[2] International Energy Agency (IEA). *Renewables 2018*.

[3] A. Alamri, M. Alowaifeer and A. P. S. Meliopoulos, "Probability Characterization of Solar Farm Power Output and Impact on System Reliability," *2018 IEEE International Conference on Probabilistic Methods Applied to Power Systems (PMAPS)*, Boise, ID, 2018, pp. 1-6.

[4] A. Alamri, M. Alowaifeer and A. P. S. Meliopoulos, "Probability Characterization of Wind Farm Power Output and Impact on System Reliability," *2018 IEEE International*

Conference on Probabilistic Methods Applied to Power Systems (PMAPS), Boise, ID, 2018, pp. 1-6.

[5] R. M. Moharil and P. S. Kulkarni, “Reliability analysis of solar photovoltaic system using hourly mean solar radiation data,” *Solar Energy*, vol. 84, no. 4, pp. 691–702, Apr. 2010.

[6] A. Bhardwaj, Vikram Kumar Kamboj, Vijay Kumar Shukla, B. Singh and P. Khurana, "Unit commitment in electrical power system- a literature review," *2012 IEEE International Power Engineering and Optimization Conference Melaka, Malaysia*, Melaka, 2012, pp. 275-280.

[7] J. Ostrowski, M. F. Anjos, and A. Vannelli, “Tight mixed integer linear programming formulations for the unit commitment problem,” *IEEE Trans. Power Syst.*, vol. 27, no. 1, pp. 39–46, Feb. 2012.

[8] S. Atakan, G. Lulli and S. Sen, "A State Transition MIP Formulation for the Unit Commitment Problem," in *IEEE Transactions on Power Systems*, vol. 33, no. 1, pp. 736-748, Jan. 2018.

[9] The U.S. Energy Information Administration (EIA), (2018). *U.S. Battery Storage Market Trends*.

[10] Oh, U.; Choi, J.; Kim, H.-H. Reliability Contribution Function considering Wind Turbine Generators and Battery Energy Storage System in Power System. *IFAC-PapersOnLine* 2016, *49*, 301–306.

[11] Wu, L.;Wen, C.; Ren, H. Reliability evaluation of the solar power system based on the markov chain method. Int. J. Energy Res. 2017, 41, 2509–2516.

[12] A. Arabali, M. Ghofrani, M. Etezadi-Amoli and M. S. Fadali, "Stochastic Performance Assessment and Sizing for a Hybrid Power System of Solar/Wind/Energy Storage," in *IEEE Transactions on Sustainable Energy*, vol. 5, no. 2, pp. 363-371, April 2014.

[13] Hasche, B. General statistics of geographically dispersed wind power. Wiley Wind Energy 2010, 13, 773–784.

[14] H. Baleriaux, E. Jamoulle, Fr. Linard de Guertechin, “Simulation de l’exploitation d’un parc de machines thermiques de production d’electricite couple a des stations de pomage”, Revue E (edition SRBE) pp 3-24, Vol V, No 7, 1967.

[15] R. R. Booth, "Power system simulation model based on probability analysis," in *IEEE Transactions on Power Apparatus and Systems*, vol. PAS-91, no. 1, pp. 62-69, Jan. 1972.

[16] S. P. Meliopoulos, "Computer-aided instruction of energy source utilization problems," in *IEEE Transactions on Education*, vol. 24, no. 3, pp. 204-209, Aug. 1981.

[17] J. Park, W. Liang, J. Choi, A. A. El-Keib, M. Shahidehpour and R. Billinton, "A probabilistic reliability evaluation of a power system including Solar/Photovoltaic cell generator," *2009 IEEE Power & Energy Society General Meeting*, Calgary, AB, 2009, pp. 1-6.

[18] R. Allan and R. Billinton, *Reliability Evaluation of Power Systems*, 1st ed. New York: Plenum, 1996.

[19] S. Mathew, *Wind energy: fundamentals, resource analysis and economics*: Berlin, Heidelberg: Springer-Verlag Berlin Heidelberg., pp. 147, 2006.

[20] K. Baker, G. Hug and X. Li, "Energy Storage Sizing Taking into Account Forecast Uncertainties and Receding Horizon Operation," in *IEEE Transactions on Sustainable Energy*, vol. 8, no. 1, pp. 331-340, Jan. 2017.

[21] R. D. Zimmerman, C. E. Murillo-Sanchez and R. J. Thomas, "MATPOWER's extensible optimal power flow architecture," *2009 IEEE Power & Energy Society General Meeting*, Calgary, AB, 2009, pp. 1-7.

[22] M. Carrion and J. M. Arroyo, "A computationally efficient mixed-integer linear formulation for the thermal unit commitment problem," in *IEEE Transactions on Power Systems*, vol. 21, no. 3, pp. 1371-1378, Aug. 2006.

[23] “System Advisor Model (SAM)", *NREL*, 2019. [Online]. Available: https://sam.nrel.gov/. [Accessed: 15- August- 2019].

[24] “Wind Prospector", *NREL*, 2019. [Online]. Available: https://maps.nrel.gov/wind-prospector. [Accessed: 22- August- 2019].

[25] S. Schoenung, “Energy storage systems cost update: A study for the DOE energy storage systems program,” Sandia Nat. Lab., Albuquerque, NM, USA, Tech. Rep. SAND2011-2730, 2011.

[26] S. A. Kazarlis, A. G. Bakirtzis and V. Petridis, "A genetic algorithm solution to the unit commitment problem," in *IEEE Transactions on Power Systems*, vol. 11, no. 1, pp. 83-92, Feb. 1996.

[27] C. Grigg *et al*., "The IEEE Reliability Test System-1996. A report prepared by the Reliability Test System Task Force of the Application of Probability Methods Subcommittee," in *IEEE Transactions on Power Systems*, vol. 14, no. 3, pp. 1010-1020, Aug 1999.